

Optical Studies of Er-doped Yttrium Aluminium Garnet Phosphor Materials

N.Norhashim
Avionics Section
Universiti Kuala Lumpur
Sepang, Malaysia
nurhakimah@unikl.edu.my

S.Kaveh
Department of Materials Science and
Metallurgy
Cambridge University
Cambridge, United Kingdom
shakiba.kaveh@gmail.com

AK Cheetham
Department of Materials Science and
Metallurgy
Cambridge University
Cambridge, United Kingdom
akc30@cam.ac.uk

RJ. Curry
Photon Science Institute
University of Manchester
Manchester, United Kingdom
richard.curry@manchester.ac.uk

Abstract— The need for materials application in solid-state lasers, medical devices, and optoelectronic devices has made the investigation of ceramic materials of increasing importance. A detail study of the optical properties of rare earth element erbium doped inside YAG is reported for the photoluminescence, power and lifetime measurement. The energy transfer and optical transitions involved for this material is studied in detail by understand the optical processes that give rise to the emission they display. Following this second (and higher) order processes are considered that lead to upconversion in erbium-doped yttrium aluminum garnet (Er:YAG) materials.

Keywords—optical properties, rare-earth material, photoluminescence

I. INTRODUCTION

The rare-earth series, often referred to as the lanthanide series have atomic numbers from 57 to 71 starting from lanthanum through to lutetium in the periodic table. The electronic configuration of the rare earth elements consists of filled 5s, 5p and 6s shell with electrons being added to the 4f shell as the series progresses. Upon bonding the rare earths tend to form trivalent ions by losing the two 6s electrons and an electron from the 4f shell [1]. As the 4f shell is shielded by the 5s² and 5p⁶ outer shells the energy levels of the 4f valence electrons is not strongly affected by the host crystal field [2] and as a result the lanthanides have sharp and well defined spectral [3][4][5].

The Y₃Al₅O₁₂ (YAG) crystalline host has superior thermal conductivity, excellent chemical stability as well as mechanical properties [6][7][8] than many other materials including glasses. Due to these properties, YAG in a single crystal form is widely used in solid state lasers as a gain host. However, single crystals are difficult to prepare in large sizes which take a long time and significant effort to grow [9]. This problem can be solved by fabricating ceramic (polycrystalline) YAG which is relatively easy to fashion into different shapes and low-cost for application such as use as phosphor or laser medium [10][11] and therefore preferred in this experiment. As a result presently most researchers are turning to the used of ceramics for future laser development. The host-material mainly influences the emission efficiency of Er³⁺ intra-atomic transitions through

the host material phonon energy. The phonon energy for the YAG material is 0.08eV [8][12][13]. For most optical applications it is important for the host material to have low phonon energy to prevent multiphonon relaxation, which allows the ion's excited states to relax through nonradiative phonon emission and indirectly leads to lower emission efficiency [14]. Although YAG (an oxide) has a higher phonon energy than fluoride crystals, its superiority in terms of mechanical hardness, thermal conductivity and optical properties make it a material of choice[8][15].

Er:YAG is useful for 1.5 μ m emission for telecommunication applications as the transmitted signal can be amplified using the erbium doped fibre amplifier (EDFA) that exploits the Er³⁺ ⁴I_{13/2} to ⁴I_{15/2} transition without the need of optical to electrical conversion of the signal. The EDFA is used to overcome losses in long-haul silica fibre transmission systems. Other than that, Er doped YAG is used in the NIR region for solid state lasers.

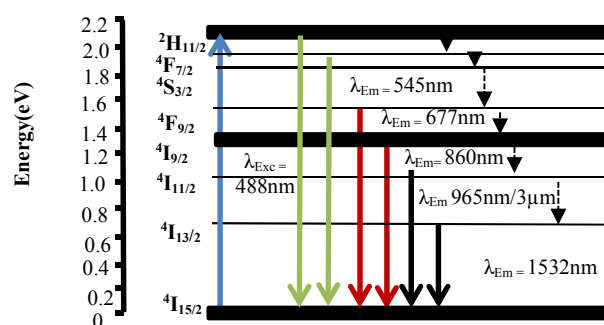


Fig 1: The energy level refers to 488nm excitation for the radiative transition and nonradiative transition. The solid blue line refers to the excitation wavelength whilst solid line (green, red and black) refer to emission wavelength. The solid lines refer to the radiative transition whilst the non-radiative transition is referring to dashed arrow.

When excited at 488nm, the Er³⁺ ion is excited to the ⁴S_{3/2} energy level. Subsequent emission is then possible a visible wavelengths centred at 545nm and in the near infrared at 965nm and 1532nm. The green emission occurs due to relaxation between the ⁴S_{3/2} to ⁴I_{15/2} levels whilst the 965nm emission is due to the ⁴I_{9/2} to ⁴I_{15/2} transition as seen in Fig. 1. For the high Er³⁺ concentrations of ~50%, ⁴I_{11/2} to ⁴I_{13/2} transition can be observed. The population density N₁ at ⁴I_{11/2}

energy level is greater than the population density N_2 $^4I_{13/2}$ which means $N_1 > N_2$, and thus a population inversion occurs. This enables amplification of photons (gain) occurring which can be used to obtain lasing. The lifetime of the upper laser level $^4I_{11/2}$ is shorter than the lower laser level at the $^4I_{13/2}$ energy level.

In the upconversion processes that occur when exciting at 980nm it is expected that green and/or red emission will result. The red emission is due to $^4I_{11/2}$ to $^4I_{15/2}$ transitions whilst the green the above mentioned $^2H_{11/2}/^4S_{3/2} \rightarrow ^4I_{15/2}$ transitions. Upconversion can take place where most Er^{3+} ions are in the first excited state. The condition consists of two excited ions in the $^4I_{13/2}$ energy level, one electron is then excited to the upper energy level $^4I_{9/2}$ and the other electron moves to the ground state, resulting in the loss of one excited ion. Upconversion can also occur through absorption of a photon by an already excited Er^{3+} ion. Since upconversion can effectively limit the maximum degree of population inversion attainable in the material, it is a crucial to understand it in the design of optical devices such as amplifiers [16]. The PL decay lifetime give further insight about the energy transfer that take place. Lifetime measurement measure the time taken for the excited state to radiatively recombine. The lifetime decay is fitted using an exponential decay function to obtain the lifetime of the PL emission as a given wavelength.

II. EXPERIMENTAL SETUP

This study uses polycrystalline YAG:Er³⁺ ceramics synthesized using a solid state reaction. In these studies two sets of ErX:YAG samples with 5 different erbium concentrations (X=2%,10%,20%,30% and 50%) are examined in Table I. The two sets of samples are labelled as fast-cooled (FC) ErX and slow-cooled(SC) ErX sample where X is the erbium doping concentration. The difference between the both samples is the rate of cooling during their synthesis. One set of samples is fast-cooled ErX from 1650°C while the other set of samples are slow-cooled ErX from 1650°C at 10°C min⁻¹. The synthesis of all samples and their structural characterization was performed by collaborators in the Prof Cheetham group at the University of Cambridge[17]. The phase separation was found for slow-cooled sample.

TABLE I: Total amount of erbium concentration in the fast-cooled (FC) and slow-cooled sample (SC)

Er concentration (Fast-cooled ErX)	Er concentration (Slow-cooled ErX)	Relative ratio of phases in slow-cooled samples (8% and 50%)
2 %	2%	-
10 %	12.2%	0.9 (8%) + 0.1(50%)
20 %	20.6%	0.7 (8%) + 0.3 (50%)
30 %	29%	0.5 (8%) + 0.5(50%)
50 %	50%	-

For photoluminescence experiments a laser source was used to excite the samples. A pulsed Nd:YAG pumped OPO laser (Spectra Physics Quanta-Ray and versaScan) source with repetition rate of 21Hz and pulse width of ~8ns was

used operating at an excitation wavelength of 980nm. The sample was held using a recessed metal plate that was covered with a quartz slide and mounted inside a cryostat with fused silica windows providing optical access (Oxford Instruments Optostat DN-V). Following excitation, emission was collected, collimated and focused using a pair of lenses (L₁ and L₂). Before the collected light was passed into a monochromator (Bentham TMc300) long pass filters (LPF) were used to prevent scattered laser light entering and detection of any second order grating reflections during measurement. For PL measurements, the standard Si or InGaAs detectors were used and the signal from the detector was sent to a lock-in amplifier (Signal Recovery DSP7265) referenced at the source repetition rate. Monochromator movement and data collection was carried out using bespoke software written in LabView. All the PL spectra collected have been corrected for the spectral response of the system. Photoluminescence lifetime measurements were performed using the same photoluminescence setup as described above.

III. RESULT AND DISCUSSIONS

2.1 PL measurement

The PL of all fast and slow-cooled samples described above were measured using 980nm excitation at various temperatures between 300K and 5K. Specifically, all the PL spectra were obtained at (i) room temperature (300K) and (ii) 77K for spectral ranges spanning 500nm-950nm and 1400-1700nm. Fig. 2(a) shows as the erbium ion increases, the PL intensity decreases due to the ion-ion quenching. Reducing the temperature to 77K does not change this trend as is seen in Fig. 2(b). There does appear to be a relative increase in the lower energy PL observed from the $^4I_{13/2}$ manifold upon reduction in temperature which reduce the electron population of the higher energy Stark levels.

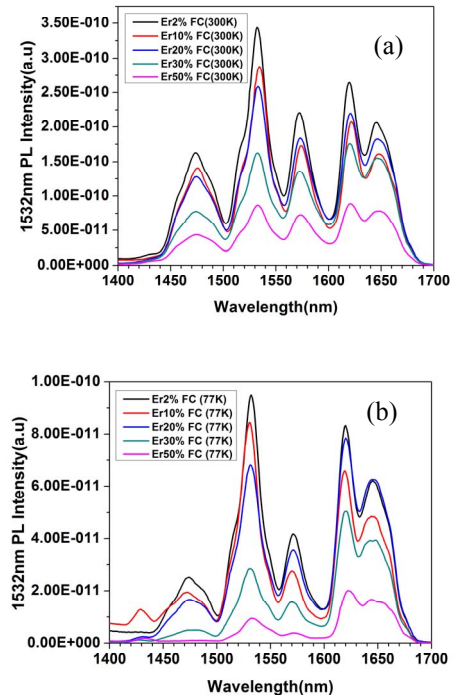


Fig. 2: The PL of fast-cooled (FC) Er:YAG samples as a function of Er concentration (2,10, 20, 30 and 50%) at 300K (a). and 77K (b). These figures indicate at 1532nm wavelength, the intensity is reduced in sequence from Er2% sample to Er50% as the temperature reduces from 300K to 77K

Excitation of the slow-cooled sample at 980nm can be referred in Fig. 3(a) and (b). At 300K the PL intensity is the highest for the Er2% sample and steadily reduces as the Er³⁺ concentration is increased to 50%. As the temperature is reduced to 77K, the PL intensity again is found not to follow the expected trend with increasing Er³⁺ concentration. Nonetheless it confirms that this behaviour is reproducible under different excitation conditions and is not an experimental artefact.

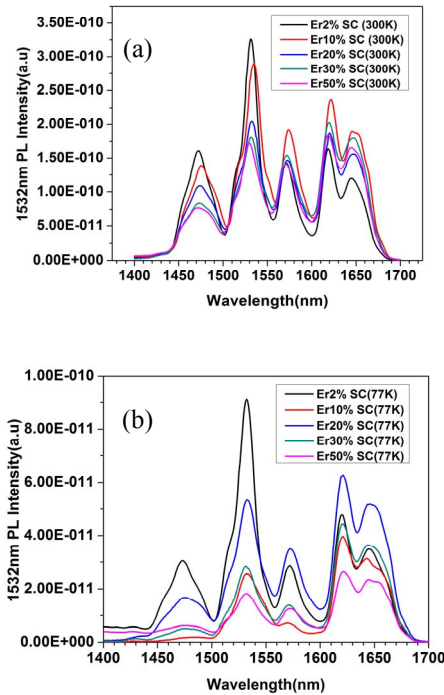


Fig. 3: The PL of slow-cooled (SC) Er:YAG samples as a function of Er concentration (2, 10, 20, 30 and 50%) at 300K (a) and 77K (b). Figure (a) indicate that the peak intensity at 1532nm reduced in sequence from Er2% to Er50% whilst figure (b) shows at 1532nm wavelength, the peak intensity reduces not following the sequences at 77K.

2.2 Lifetime measurement

Considering the 1532nm emission lifetime, all fast-cooled samples display bi-exponential decay with a general reduction in both (τ_1 and τ_2) with decreasing temperature. The Er30% and 50% samples display only a small temperature dependence which indicates that ion-ion interactions dominate the quenching processes. Comparing the fast-cooled and slow-cooled samples at 300K it is found that the slow-cooled Er2% sample has a longer lifetime at 300K than the fast-cooled. This trend is reversed for the Er50% samples with the fast-cooled sample displaying the longer lifetime, Table II. At intermediate Er concentrations no clear pattern is found at 300K which may, for the slow-cooled samples, be related to the percentage of the erbium ion in each phase and will be discussed later. At 5K the slow-cooled samples typically have a shorter lifetime than the fast-cooled samples of the same Er concentration with the exception of the Er30% sample. At room temperature, Er2% fast-cooled sample shows a small variation in τ_2 compared to the Er2% slow-cooled sample may be due to the experimental artefact during the measurement. Likewise, other variations can be found (e.g. for the Er30% samples) that are related to the percentage of Er rich and Er deficient regions. The lifetime of Er30% is decrease if compared to Er20% which is an indication of other processes (e.g. ETU)

starting to impact. For the Er50% fast-cooled and slow-cooled samples two different lifetimes are found which may indicate that for the Er50% slow-cooled sample 3um emission is more probable, as so explaining the 1532nm lifetime reduction.

TABLE II: The summary of the lifetime different between the fast-cooled and slow-cooled sample for τ_1 and τ_2 at 980nm excitation.

Sample	5K		300K	
	τ_1 (μ s)	τ_2 (μ s)	τ_1 (μ s)	τ_2 (μ s)
Er2%(FC)	4910	1940	5140	1830
Er2%(SC)	4510	1780	5230	2020
Er10%(FC)	2690	1070	3610	1300
Er10%(SC)	2450	880	3420	1290
Er20%(FC)	2840	577	3950	837
Er20%(SC)	2660	678	3760	969
Er30%(FC)	1920	482	2080	614
Er30%(SC)	2210	517	2730	656
Er50%(FC)	1980	354	2160	415
Er50%(SC)	859		972	290

Fig. 4(a) and (b) shows the upconversion PL for fast-cooled ErX (X = 10, 20, 30 and 50%) samples under 980nm excitation obtained at 300K and 77K. Three main emission bands are found centred at 545nm (⁴S_{3/2}-⁴I_{15/2}), 677nm (⁴I_{9/2}-⁴I_{15/2}) and 864nm (⁴I_{9/2}-⁴I_{15/2}). At 300K, as the erbium concentration increases the upconversion PL intensity increases with Er30% showing the highest intensity. As the temperature is reduced to 77K, the Er50% shows the highest intensity especially at 677nm and 864nm where little difference in intensity of found for the other samples. The Er2% sample was found not to display upconversion.

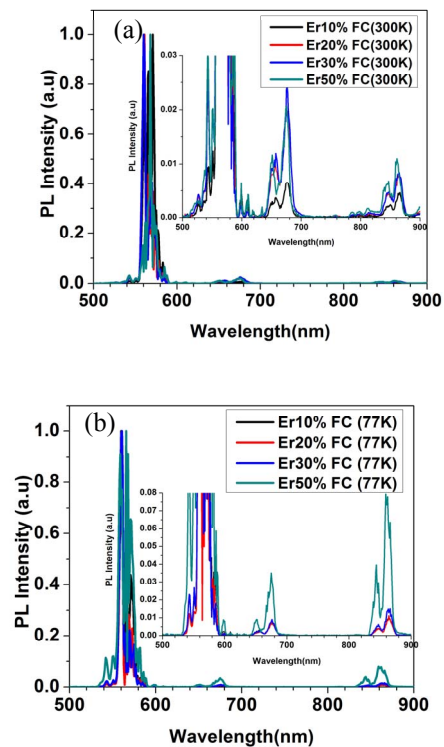


Fig. 4: Upconversion photoluminescence of 980nm excited fast-cooled (FC) samples at 300K (a) and 77K (b). Figure (a) shows that at 677nm and 864nm wavelength Er30% has the highest intensity at 300K whilst as the temperature reduces, the Er50% has the highest intensity at 77K.

Fig 5(a) and (b) shows the upconversion PL obtained from the slow-cooled samples again at 300K and 77K and the same three emission bands observed as above. At 300K, the upconversion increases in intensity in line with the erbium concentration. This contrasts the 1532nm emission which displays the highest intensity for the lowest Er concentration samples. This provides support for the above observations of quenching being linked to ion-ion interactions of which upconversion is one outcome. As the temperature is reduced to 77K, Er30% shows the strongest upconversion unlike what was found for the fast-cooled samples. This deviation between the behaviour of the fast and slow-cooled samples is indicative of the phase separation seen in these samples.

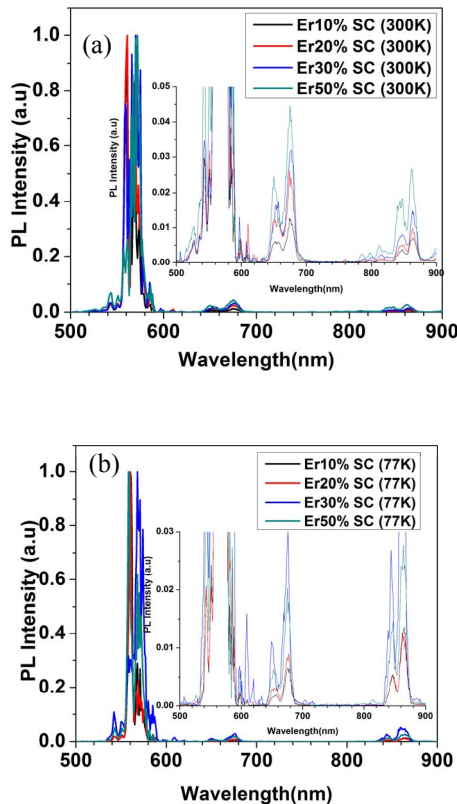


Fig. 5: Upconversion photoluminescence of 980nm excited slow-cooled samples at 300K (a) and 77K (b). Figure (a) indicates that the upconversion increases in intensity in line with the erbium concentration. As the temperature reduce to 77K figure (b) indicate that Er30% shows the strongest upconversion.

The two principle mechanisms involved for achieving upconversion emission rely on high excited state populations of the $^4I_{11/2}$ or $^4I_{13/2}$ energy levels:

$$(a) \text{ ESA: } ^4I_{11/2} \rightarrow ^4F_{7/2} \quad (\text{Route A})$$

$$(b) \text{ ETU: } ^4I_{15/2} \rightarrow ^4I_{11/2}, ^4I_{13/2} \rightarrow ^4F_{9/2} \quad (\text{Route B})$$

ESA is able to directly populate the $^4F_{7/2}$ energy level from which green emission may result. ETU is not able to produce green emission but may lead to red upconversion emission from the $^4F_{9/2}$ level. Both of these processes are in effect 2-photon (nonlinear) mechanisms. These are shown in Fig. 6 with route A (ESA) found to be more efficient at leading to green emission than red. Route B of course may only lead to red emission [18]. All fast-cooled and slow-cooled samples

display upconversion with the exception of Er2% due to the reduced ion-ion interaction in this sample.

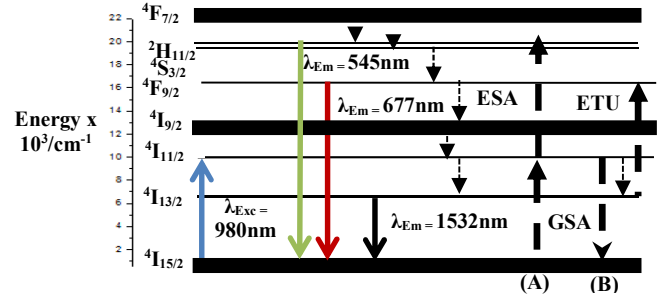


Fig. 6: Schematic energy level diagram for Er^{3+} ions under 980 nm excitation for visible and NIR emission. The blue arrow (solid line) show the excitation wavelength whilst the other colours (solid lines) are the emission wavelength. The dashed arrow shows the nonradiative energy transfer whilst the dotted arrow show the multiphonon relaxation.

Previous studies have reported upconversion in the Er:YAG samples [19][18][20]. In order to understand the contribution of such two-photon process we studied the pump power dependence of the green and red upconversion emission intensity. The data is fitted using the log-lin plot in order to extract the value of n which gives the average number of the photons absorbed per upconverted photon emitted. Comparing the relative intensities of the upconverted green and red emission it is found that the green has ~ 5 times greater intensity than the red (Table III) and this is true for both samples. As such this indicates that route A dominates over route B as the principle mechanism for obtaining upconversion. As the Er concentration is increased the relative strength of the green upconversion emission is reduced. If the number of n is obtained more than two, it more than one process which is expected as both routes A and B may contribute to red emission [21].

TABLE III: The value of n for green and red emission fast-cooled and slow-cooled sample

Erbium concentration (ErX)	Red n value (300K)	Green n value(300K)
Fast-cooled Er10	1.83 (UC)	0.53
Slow-cooled Er10	2.38 (UC)	0.41
Fast-cooled Er20	2.65 (UC)	0.53
Slow-cooled Er20	2.35 (UC)	0.62
Fast-cooled Er30	2.49 (UC)	0.90
Slow-cooled Er30	2.07 (UC)	-0.01
Fast-cooled Er50	2.28 (UC)	-0.06
Slow-cooled Er50	2.02 (UC)	0.25

Fig. 7 plots the red upconversion emission intensity as a function of Er concentration. As expected the intensity increases with concentration as ion-ion interactions become more probable. The fast-cooled samples indicate that there is a temperature dependence which is most prominent at an Er concentration of 30%. The slow cooled samples show no such dependence. It is typically found that optimum ETU occurs when the erbium concentration is between 20-30% as above these concentrations other non-radiative ion-ion interactions start to dominate. This is indeed the trend observed within the fast-cooled samples at room temperature with the Er50% having reduced red upconversion emission. That this is not seen in the slow-cooled samples is related to

the bi-phasic nature of the Er concentrations. As mentioned above, the bi-phasic samples consist of an 8% and 50% Er-rich phase. As a result neither phase is optimal for obtaining upconversion even though the overall Er concentration may be 'ideal'. This therefore accounts for the variations observed in behaviour between the samples and re-iterates the importance of understanding and controlling sample preparation when synthesis the phosphors.

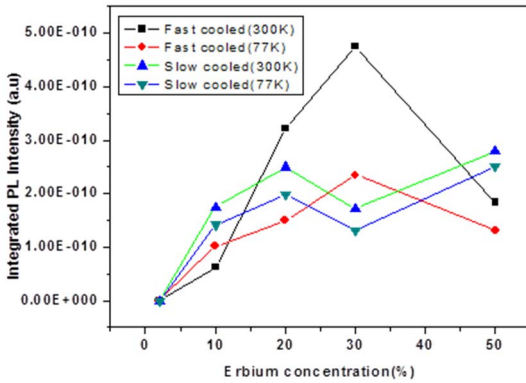


Fig. 7: The intensity of red upconversion emission as a function of erbium concentration at 300K and 77K. The above figure indicate that Er30% FC (black colour) has the highest PL intensity at 300K whilst the Er30% SC (blue colour) has the lowest intensity at 300K

The upconversion emission when exciting at 980nm directly competes with 1532nm emission as an effective alternative relation mechanism and is therefore deleterious. Fig. 8(a) and (b) shows the integrated 1532nm PL intensity as a function of Er concentration under 980nm excitation.

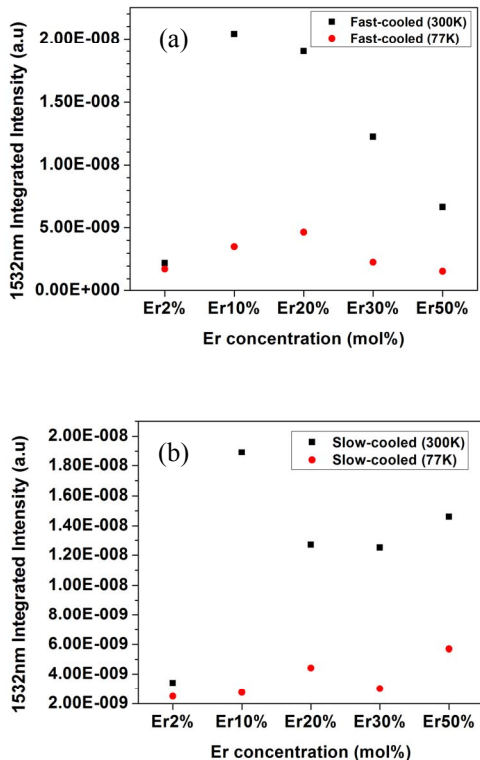


Fig. 8: The integrated intensity of 1532nm emission as a function of erbium concentration at 300 and 77K for (a) fast-cooled sample (b) slow-cooled sample. Figure (a) indicates the emission at 1532 nm, the PL intensity decreases linearly as the temperature is reduced.

Emission at 1532 nm, the PL intensity decreases linearly as the temperature is reduced. This is may be due to the 980nm excited $^4I_{11/2}$ level relaxing non-radiatively to the $^4I_{13/2}$ level followed by a second photon upconverting the excited state to $^4F_{9/2}$. From this state non-radiative relaxation through the $^4F_{9/2} \rightarrow ^4I_{11/2} \rightarrow ^4I_{13/2} \rightarrow ^4I_{15/2}$ levels may occur, eventually giving 1532 nm emission. In the process excitation energy required and the second photon energy are slightly mismatched however and therefore in order for ET to occur a phonon is required. As the temperature is decreased so is the phonon population and the ET becomes less probable resulting in the PL intensity also being reduced.

Inspection of the 980nm excited 1532nm emission lifetime measurements Fig. 9(a) and (b) shows that as the erbium concentration increases the PL lifetime reduces for both fast and slow-cooled samples. This is due to the energy transfer that takes place [21] including the ETU discussed above. Other studies have found similar results with PL quenching and a reduction in the lifetime being observed [22][23].

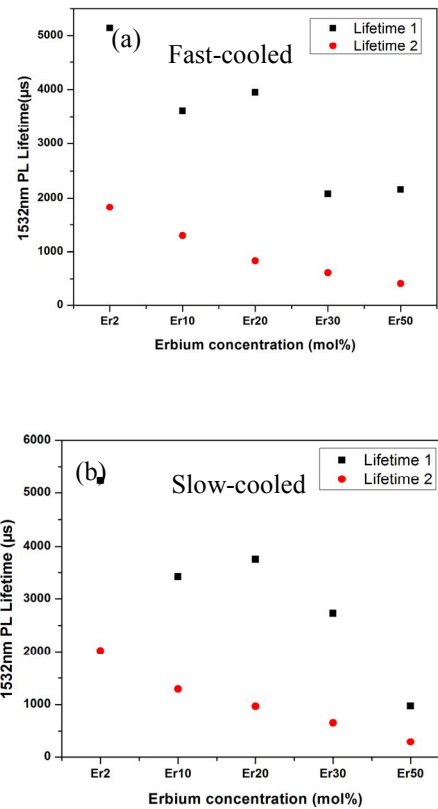


Fig. 9: The 980nm excited 1532nm PL lifetime as a function of erbium the fast concentration for fast-cooled (a) and slow-cooled (b) samples. Both figures indicate that as the erbium concentration increases the PL lifetime reduces for both fast and slow-cooled samples.

IV. CONCLUSION

The optical properties of Er:YAG were investigated as a function of Er concentration, temperature and excitation power dependence. It is generally observed that the two types of sample have slightly different optical properties resulting from the bi-phasic nature of the Er concentration in the slow-cooled samples. This presents difficulties in clearly resolving the dominant mechanisms that govern the emission

obtained from the samples but clearly indicate that sample preparation is critical if consistent performance is to be achieved. The upconversion emission at 545nm and 677nm was observed which in the bi-phasic samples is reduced and therefore may assist in improving the yield of 1532nm emission and also 3 μ m emission. This later emission may be strongly affected by the ETU process and therefore has important implications on the performance of Er:YAG 3 μ m lasers. In these devices an erbium concentration of 40-50% is required to obtain strong ETU from the $^4I_{13/2}$ level which then reduce the lifetime of the 1532 nm emission. This is required in order to achieve a population inversion of the $^4I_{11/2}$ from which the 3 μ m emission occurs. As a conclusion, mono-phasic and bi-phasic Er:YAG samples can be used as a potential material for obtaining emission. Careful choice of material, based on synthesis, may enable improved performance by either promoting or reducing ion-ion interactions. Equally, lack of control over the synthesis may lead to unforeseen deleterious effects due to phase separation.

REFERENCES

- [1] L. R Tessler and A.C Iniguez, "Optimization of the as-deposited 1.54 μ m photoluminescence intensity in a-SiO_x H(Er)" 269 603–607 2000
- [2] J.C.G. Bünzli and S.V Eliseeva "Lanthanide NIR luminescence for telecommunications, bioanalyses and solar energy conversion" *J. Rare Earths* 28(6) 824–842 2010
- [3] R Scheps "Upconversion Laser Processes" Elsevier Sci. Ltd.20 (4) 271–358 1996
- [4] B. M. Walsh "Judd-ofelt Theory: Principles and Practices " 403–433 2006
- [5] J Garcia Sole, L Bausa, and D Jaque *An Introduction to the Optical Spectroscopy of Inorganic Solids* 2005
- [6] N Ter-Gabrielyan, M Dubinskii, G.A Newburgh, A Michael and L.D Merkle "Temperature dependence of a diode-pumped cryogenic Er:YAG laser *Opt. Express*" 17(9) 7159–69 2009
- [7] B Denker et al. "Yb³⁺,Er³⁺:YAG at high temperatures: Energy transfer and spectroscopic properties" *Opt. Commun.* 271(1) 142–147 2007
- [8] F Cornacchia et al. "Growth and spectroscopic properties of Er:YAG crystalline fibers" *J. Cryst. Growth* 275 534–540 2005
- [9] M Liu, S.W Wang, D.Y Tang, L.D Chen, and J Ma "Fabrication and microstructures of YAG transparent ceramics" *Sci. Sinter* 40 311–317 2008
- [10] G Qin et al. "Upconversion luminescence of Er³⁺ in highly transparent YAG ceramics" *Solid State Commun* 132(2) 103–106 2004
- [11] S Hinojosa, O Barbosa-García, M.A Meneses-Nava, J.L Maldonado, Ede la Rosa-Cruz, and G. Ramos-Ortiz "Luminescent properties and energy transfer processes of co-doped Yb–Er poly-crystalline YAG matrix" *Opt. Mater. (Amst)*. 27(12) 1839–1844 2005
- [12] L Aarts, S Jaeqx, B.M Van der Ende and A Meijerink "Downconversion for the Er³⁺, Yb³⁺ couple in KPb₂Cl₅—A low-phonon frequency host" *J. Lumin.*131(4) 608–613 2011
- [13] T Kushida, S Kinoshita, T Ohtsuki, and T Yamada "Multiphonon Relaxation Rate from Pumped Level to Upper Laser Level in YAG:Nd" 44(9) 1363–1365 1982
- [14] C Strümpel et al. "Modifying the solar spectrum to enhance silicon solar cell efficiency—An overview of available materials" *Sol. Energy Mater. Sol. Cells* 91(4) 238–249 2007
- [15] H. L Xu and S Kröll 2005 Upconversion dynamics in Er³⁺-doped YAG *J.Lumin.*111(3) 191–198
- [16] F Enrichi and E Borsella "A simple approach for upconversion determination using low excitation power:The photoluminescence analysis of an Er-doped aluminosilicate glass" *Materials Science and Engineering B: Solid-State Materials for Advanced Technology* 105 20–24 2003
- [17] S Kaveh, C.P Tremblay, N Norhashim, R.J.Curry, and A. K. Cheetham "Phase separation in garnet solid solutions and its effect on optical properties". *Adv. Mater* 25 6448–52 2013
- [18] J Zhou, W Zhang, J Li, B Jiang, W Liu, and Y Pan "Upconversion luminescence of high content Er-doped YAG transparent ceramics" *Ceram. Int.* 36(1) 193–197 2010
- [19] E Cavalli, L Esposito, J Hostaša, and M Pedroni "Synthesis and optical spectroscopy of transparent YAG ceramics activated with Er³⁺" *J. Eur. Ceram. Soc.* 33(8) 1425–1434 2013
- [20] G Qin et al. "Upconversion luminescence of Er³⁺ in highly transparent YAG ceramics" *Solid State Commun* 132(2) 103–106 2004
- [21] M Pokhrel et al. "Infrared and upconversion spectroscopic studies of high Er³⁺ content transparent YAG ceramic" *Optical Materials Express* 1 1272 2011
- [22] S Du, L Jiang, W Zhang, X Dong, and Z Dai "Sensitivities of competitions between different upconversion mechanisms to exciting wavelength in Er³⁺:YAG with different concentrations" *Opt. Commun.* 284(14) 3593–3596 2011
- [23] W.Q Shi, M Bass, and M Birnbaum "Effects of energy transfer among Er³⁺ ions on the fluorescence decay and lasing properties of heavily doped Er:Y₃Al₅O₁₂" *J.Opt. Soc. Am. B* 7(8) 1456 1990